ACS Chemical Neuroscience

Research Article

Cite This: ACS Chem. Neurosci. 2017, 8, 2549-2557

pubs.acs.org/chemneuro

Placement of Hydroxy Moiety on Pendant of Peptidomimetic Scaffold Modulates Mu and Kappa Opioid Receptor Efficacy

Aubrie A. Harland,[†] Irina D. Pogozheva,[†] Nicholas W. Griggs,[‡] Tyler J. Trask,[‡] John R. Traynor,[‡] and Henry I. Mosberg*[,†,§]

[†]Department of Medicinal Chemistry, College of Pharmacy, University of Michigan, Ann Arbor, Michigan 48109, United States

[‡]Department of Pharmacology, Medical School, University of Michigan, Ann Arbor, Michigan 48109, United States

[§]Interdepartmental Program in Medicinal Chemistry, University of Michigan, Ann Arbor, Michigan 48109, United States

Supporting Information

ABSTRACT: In an effort to expand the structure−activity relationship (SAR) studies of a series of mixed-efficacy opioid ligands, peptidomimetics that incorporate methoxy and hydroxy groups around a benzyl or 2-methylindanyl pendant on a tetrahydroquinoline (THQ) core of the peptidomimetics were evaluated. Compounds containing a methoxy or hydroxy moiety in the *o*- or *m*-positions increased binding affinity to the kappa opioid receptor (KOR), whereas compounds containing methoxy or hydroxy groups in the *p*-position decreased KOR affinity and reduced or eliminated efficacy at the mu opioid receptor (MOR). The results from a substituted 2-methylindanyl series aligned with the findings from the substituted benzyl series. Our studies culminated in the development of **8c**, a mixed-efficacy MOR agonist/KOR agonist with subnanomolar binding affinity for both MOR and KOR.

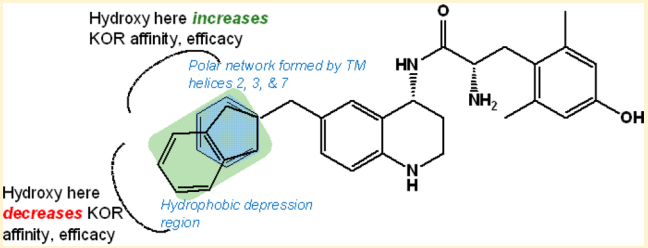

KEYWORDS: *Mixed-efficacy opioid ligands, kappa opioid receptor agonist, mu opioid receptor agonist, peptidomimetics, structure−activity relationships*

INTRODUCTION

Over the last two decades many studies have shown the potential clinical utility of dual-acting opioid agents, suggesting that the opioid receptors do not act independently of each other and that modulation of one receptor type affects the activation of other opioid receptor types. In the opioid field, there are important implications for several emerging mixed-efficacy profiles. For example, opioid ligands with a mixed-efficacy mu opioid receptor (MOR) agonist/delta opioid receptor (DOR) antagonist profile have shown promise in the development of analgesics with reduced tolerance and dependence liabilities.[1−3] Likewise, studies have shown that administration of a sub-antinociceptive dose of a DOR agonist in combination with a MOR agonist can increase the potency of a MOR agonist in animal models.[4,5] Furthermore, there are indications of clinical utility of mixed-efficacy MOR/kappa opioid receptor (KOR) ligands. For example, accumulating evidence suggests that a mixed-efficacy MOR antagonist/KOR agonist, such as nalbuphine, could be used in the treatment of cocaine addiction.[6] Additional studies have shown that concomitant administration of a MOR partial agonist with a KOR agonist produces additive analgesia with reduced respiratory depression, tolerance, and dependence.[7,8] More recently, there is evidence that the dual-acting KOR agonist/DOR agonist **MP1104** not only produces antinociception while lacking the rewarding and dysphoric effects but is also capable of blocking cocaine conditioned place preference in mice implicating KOR/DOR ligands as an emerging profile to treat pain and cocaine addiction.[9] Thus, the emerging evidence suggests that simultaneous modulation of two or more opioid receptors may provide analgesics with reduced liability for producing tolerance and dependence and could serve as treatments in other disease states.

We have previously described a series of opioid peptidomimetics, based on a tetrahydroquinoline (THQ) scaffold, that exhibit a MOR agonist/DOR antagonist profile[10−12] as potential analgesics devoid of tolerance and dependence liabilities, as well as a series of compounds that produce a MOR agonist/DOR partial agonist profile.[13] After completing SAR campaigns that examined the effects of changes to the original peptidomimetic THQ core,[10] which included implementing a tetrahydronapthalene (THN) core,[11] incorporating various *N*-substitutions on the THQ core,[11,13] and exploring different pendant moieties,[12] we set out to do a smaller, more focused SAR campaign concentrating on small substitutions on the pendant. Here we examine the effect of methoxy and hydroxy moieties on benzyl and 2-methylindanyl pendants attached to the THQ scaffold (Figure 1). These pendants were

Received: July 21, 2017
Accepted: August 10, 2017
Published: August 10, 2017

DOI: 10.1021/acschemneuro.7b00284
ACS Chem. Neurosci. 2017, 8, 2549−2557

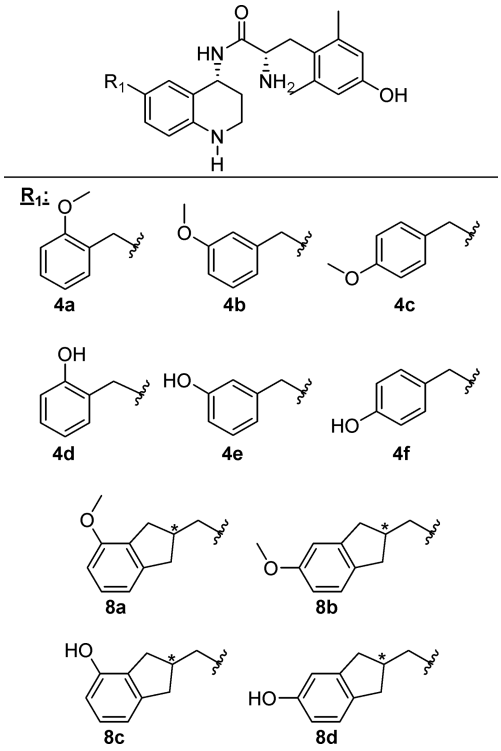

Figure 1. Peptidomimetic analogues.

chosen, in particular, because both are easily modified at individual carbon atoms for methodical SAR studies probing a range of chemical space. Moreover, the 2-methylindanyl analogues served as probes to determine the spatial depth of this area of the receptor binding pocket. In addition, the methoxy and hydroxy analogue pairs help map the hydrogen-bonding requirements and networks in this area of the binding pocket. With this synthetic approach, it was our goal to exploit minor differences in the MOR, DOR, and KOR binding pockets that could help tailor binding and efficacy profiles across all three receptors (Figure 1).

Through this synthetic campaign, we unexpectedly uncovered a subset of peptidomimetic ligands with a range of mixed-efficacy MOR agonist/KOR agonist profiles. Although reports of mixed-efficacy MOR/KOR ligands exist in the literature, none of the reported compounds share a common structural motif with the THQ scaffold (Figure 2). Until recently, most KOR ligands in the literature incorporate morphinan, benzomorphan, or oripavine scaffolds, or in the case of salvinorin A, a diterpenoid scaffold (Figure 2). There are, however, select KOR ligands that do not incorporate one of these common scaffolds and include such ligands as JDTic[14] and U69,593,[15] which are both high affinity KOR ligands. Recently, interest in the development of novel KOR ligands[16−19] has surged, and many groups are now focused on generating mixed-efficacy[20−22] ligands or biased ligands[23] at KOR. Such mixed-efficacy or biased ligands with distinct scaffolds could provide analgesia while attenuating certain side effects seen with MOR agonist ligands as well as those associated with full KOR agonists, for example, dysphoria. Herein, we report a novel SAR study using our peptidomimetic scaffold for the development of mixed-efficacy MOR/KOR ligands.

RESULTS

Synthesis of the Substituted Benzyl Analogues, 4a−4f. Synthesis of the methoxy- and hydroxybenzyl analogues began with a Suzuki coupling between **1** (the synthesis of which

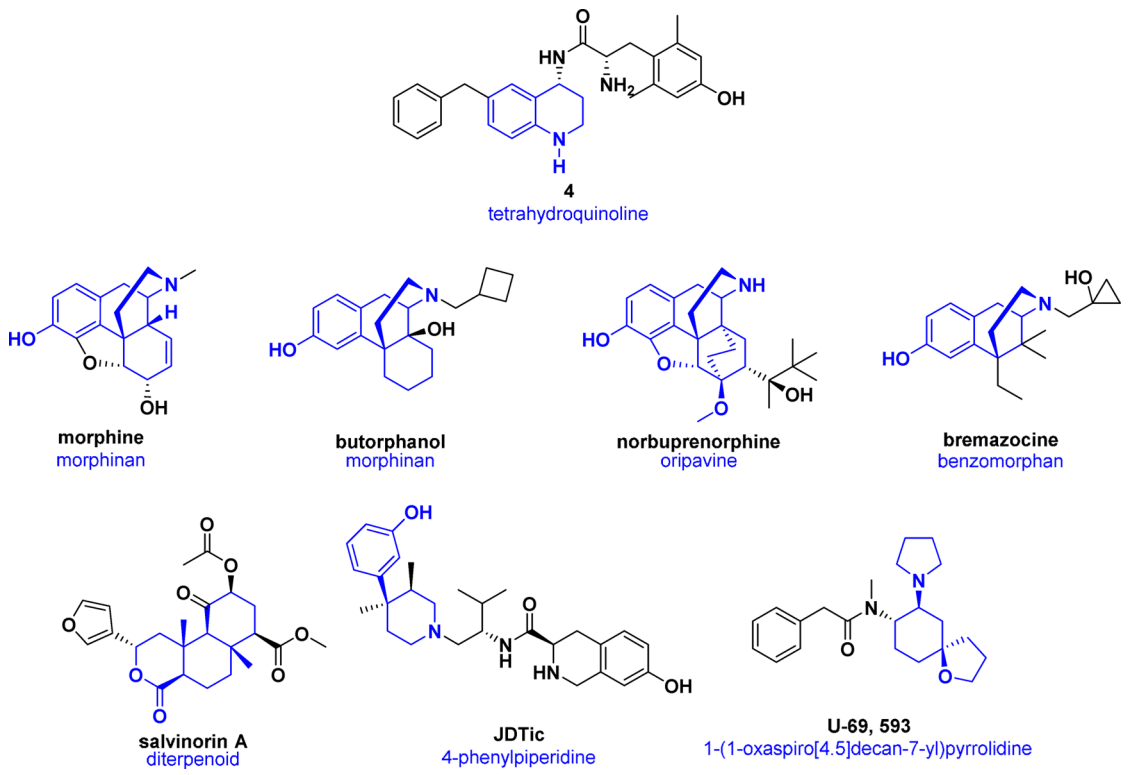

Figure 2. Representative examples of common scaffolds in kappa opioid receptor ligands.

DOI: 10.1021/acschemneuro.7b00284
ACS Chem. Neurosci. 2017, 8, 2549−2557

Scheme 1. Synthesis of the Substituted Benzyl Analogues[a]

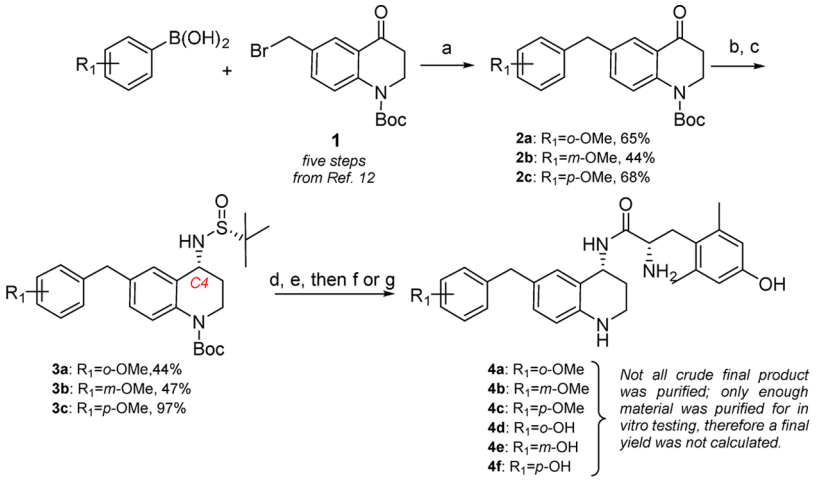

[a](a) R-B(OH)$_2$, Pd(dppf)Cl$_2$, K$_2$CO$_3$, 3:1 acetone/H$_2$O, MW 100 °C, 300 W; (b) (*R*)-*t*-butanesulfinamide, THF, Ti(OEt)$_4$, 0 °C then reflux at 75 °C; (c) NaBH$_4$, THF, −50 °C to RT, 3 h, then MeOH, RT; (d) HCl, dioxane, RT, 3 h; (e) diBoc-Dmt, PyBOP, 6Cl-HOBt, DIPEA, DMF, RT; (f) 1:1 TFA/DCM (for **4a**−**4c**); (g) BBr$_3$, DCM, 2 h, then MeOH (for **4d**−**4f**).

Scheme 2. Synthesis of the 2-Methylindanyl Analogues

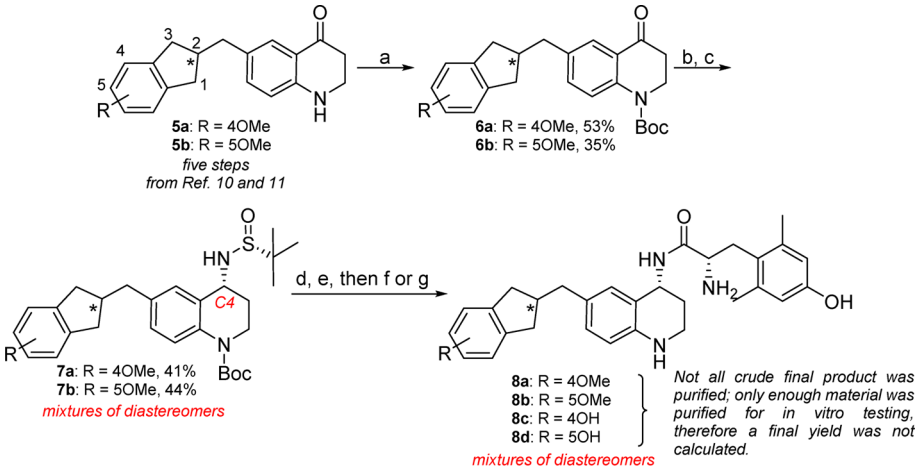

[a](a) Boc$_2$O, DMAP, DIPEA, DCM, 60 °C; (b) (*R*)-*t*-butanesulfinamide, THF, Ti(OEt)$_4$, 0 °C, then reflux at 75 °C; (c) NaBH$_4$, THF, −50 °C to RT, 3 h, then MeOH, RT; (d) HCl, dioxane, RT, 3 h; (e) diBoc-Dmt, PyBOP, 6Cl-HOBt, DIPEA, DMF, RT, 6 h; (f) 1:1 TFA/DCM, RT, 1 h (for **8a** and **8b**); (g) BBr$_3$, DCM, 2 h, then MeOH (for **8c** and **8d**).

has been previously published[12]) and the commercially available methoxybenzyl boronic acid to form **2a**−**2c**. Treatment of **2a**−**2c** with (*R*)-*t*-butanesulfinamide and Ti(OEt)$_4$ yielded imines *in situ*, which were then reduced with NaBH$_4$ to form **3a**−**3c** with the desired *R*-stereochemistry at the C4 position.[24−26] The Ellman auxiliary of **3a**−**3c** was cleaved using concentrated HCl, forming the primary amine salts,[24] which were then coupled to diBoc-Dmt and subsequently deprotected with either trifluoroacetic acid (TFA) to yield compounds **4a**−**4c** or BBr$_3$ to yield **4d**−**4f** (Scheme 1).

Synthesis of the Substituted 2-Methylindanyl Analogues, 8a−8d. For the synthesis of the 2-methylindanyl analogues, the pendant moiety was incorporated in the first step using chemistry that was previously published.[10,11] Briefly, an aldol condensation between 4- or 5-methoxy-1-indanone and *p*-nitrobenzaldehyde yielded the *p*-nitro aldol adduct, which was hydrogenated to yield the 4-(2-methylindanyl)-anilines. The anilines were acylated with 3-bromopropionyl chloride, cyclized to form lactams, and then treated with trifluoromethanesulfonic acid (TfOH) to promote a Fries rearrangement and yield **5a** and **5b**, as described by Schmidt et al.[27] (See Supporting Information for full experimental data). Intermediates **5a** and **5b** were Boc-protected forming intermediates **6a** and **6b**.[10] Intermediates **6a** and **6b** were treated with (*R*)-*t*-butanesulfinamide and Ti(OEt)$_4$ to yield imines *in situ*, which were reduced with NaBH$_4$ to form the desired *R*-stereochemistry at C4 of intermediates **7a** and **7b**.[24−26] The Ellman auxiliary was cleaved using concentrated HCl, forming primary amine salts,[24] which were then coupled to diBoc-Dmt and subsequently deprotected using TFA to yield compounds **8a** and **8b**. Analogues **8c** and **8d** were synthesized by using BBr$_3$ (Scheme 2).

Opioid Receptor Binding and Efficacy. Analogues **4a**−**4f** and **8a**−**8d** were evaluated in *in vitro* by performing MOR, DOR, and KOR binding and efficacy assays, as previously described[28−30] (Table 1). Binding affinities (K_i (nM)) were obtained by competitive displacement of radiolabeled [^{3}H]-diprenorphine in membrane preparations from C6 cells stably

DOI: 10.1021/acschemneuro.7b00284
ACS Chem. Neurosci. 2017, 8, 2549−2557

Table 1. Binding Affinity and Efficacy Data for Peptidomimetics

		Binding, K_i (nM)[a,c]			EC_{50} (nM)[b,c]			% stimulation [b,c]		
Cmpd	R	MOR	DOR	KOR	MOR	DOR	KOR	MOR	DOR	KOR
4[e]		0.22 (0.02)	9.4 (0.8)	68 (2)	1.6 (0.3)	110 (6)	540 (72)	81 (2)	16 (2)	22 (2)
4a		0.34 (0.08)	6.5 (2.2)	54 (14)	8.9 (1.8)	130 (14)	1000 (440)	91 (6.5)	16 (2.2)	9.6 (1.1)
4b		0.11 (0.03)	5.4 (1.0)	27 (3.4)	4.4 (0.57)	230 (8.5)	dns[d]	99 (1.7)	10 (2.6)	dns[d]
4c		0.29 (0.04)	15 (1.1)	100 (19)	9.3 (1.9)	dns[d]	dns[d]	55 (3.4)	dns[d]	dns[d]
4d		0.26 (0.04)	5.6 (2.5)	5.7 (1.4)	9.8 (4.2)	1500 (700)	270 (15)	89 (2.6)	21 (2.2)	67 (3.5)
4e		0.19 (0.02)	1.4 (0.17)	16 (2.8)	4.8 (0.43)	140 (4.5)	230 (67)	96 (4.8)	67 (1.6)	17 (1.4)
4f		1.7 (0.35)	130 (21)	420 (27)	dns	dns[d]	dns[d]	dns	dns[d]	dns[d]
8[e]		0.16 (0.04)	4.1 (2)	1.2 (0.4)	0.24 (0.03)	dns	68 (15)	86 (1)	dns	38 (2)
8a		0.09 (0.00)	2.3 (0.87)	67 (3.6)	1.9 (0.51)	dns[d]	dns[d]	48 (2.9)	dns[d]	dns[d]
8b		0.08 (0.03)	6.2 (1.5)	33 (8.4)	7.9 (3.6)	dns[d]	dns	22 (3.7)	dns[d]	dns
8c		0.18 (0.03)	6.0 (1.3)	0.77 (0.09)	4.9 (1.2)	dns[d]	25 (4.0)	66 (3.3)	dns[d]	92 (3.6)
8d		0.82 (0.09)	15 (0.79)	41 (1.5)	7.0 (1.1)	dns	dns	16 (2.4)	dns	dns

[a]Binding affinities (K_i (nM)) were obtained by competitive displacement of radiolabeled [^{3}H]-diprenorphine in membrane preparations. [b]Efficacy data were obtained using agonist induced stimulation of [^{35}S]-GTPγS binding. Efficacy is represented as percent maximal stimulation relative to standard agonist DAMGO (MOR), DPDPE (DOR), or U69,593 (KOR) at 10 μM. Potency (EC_{50} (nM)) is calculated from the percent maximal stimulation as the concentration of drug required to produce half the maximal stimulation. [c]All values are expressed as the mean with SEM in parentheses for n = 3 independent assays in duplicate, unless otherwise noted. [d]n = 2 independent assays in duplicate. dns: does not stimulate. [e]Published in ref 10.

expressing rat MOR (C6-MOR) or rat DOR (C6-DOR) or CHO cells stably expressing human KOR (CHO-KOR), as previously described[28,29] (Table 1). Efficacy data were obtained using agonist-induced stimulation of [^{35}S]-GTPγS binding to G protein[28] in the same cell preparations as previously mentioned. Relative efficacy was quantified as percent maximal stimulation relative to standard agonist (DAMGO at MOR, DPDPE at DOR, and U69,593 at KOR). Analogue potency (EC_{50} (nM)) was calculated as the concentration of drug required to produce half the observed maximal stimulation (Table 1).

The methoxy- and hydroxybenzyl subseries offers insight into the electronic limitations and requirements in the pendant binding region of the receptors. First and foremost, binding affinities at MOR and DOR for compounds with *o*- or *m*-methoxy and hydroxy substitutions (**4a**, **4b**, **4d**, and **4e**) remain relatively unchanged when compared to the unsubstituted benzyl analogue, **4** (Table 1), indicating that H-bond donors and acceptors are tolerated in these regions of the three opioid receptors. Compound **4f** with a *p*-hydroxy showed reduced binding affinity to all three opioid receptors especially at DOR and KOR, while **4c** with a *p*-methoxy group had reduced binding to KOR. In contrast, binding affinity to KOR increased for both **4d** with the *o*-hydroxy (K_i = 5.7 nM) and **4e** with the *m*-hydroxy (K_i = 16 nM) but not for the corresponding methoxy analogues **4a** (K_i = 54 nM) and **4b** (K_i = 27 nM), as compared to **4** (K_i = 68 nM). This observation suggests a possible role of a hydrogen bond donor, rather than an acceptor, at the *o*- or *m*-position of the benzyl pendant for improved ligand binding to KOR.

The profile of ligand efficacy for the benzyl subseries was more complex. Most compounds were MOR agonists with relatively high efficacy and nanomolar potency at MOR, except **4f** with *p*-hydroxy, which was an apparent antagonist (no stimulation of GTP binding) with nanomolar binding affinity. In contrast, at DOR, most compounds from this subseries were either partial agonists with 10−20% efficacy (**4**, **4a**, **4b**, **4d**) or did not stimulate GTPγS binding (**4c**, **4f**), except **4e** with *m*-hydroxy, which demonstrated increased efficacy (67% stimulation) but low potency (EC_{50} = 140 nM). We have previously shown that compounds in this peptidomimetic series that do not stimulate GTPγS binding do in fact act as functional antagonists as demonstrated by a shift in the dose−response curves of standard agonists.[10,12] This was confirmed here for the representative **4f**, which was observed to shift the dose response curves of DPDPE at DOR (K_e = 430 nM) and of DAMGO at MOR (K_e = 810 nM). Similar to the observations at DOR, at KOR, the majority of these ligands were either partial agonists with low potency (**4**, **4a**, **4e**) or displayed no agonist effect (**4b**, **4c**, **4f**), except **4d** with *o*-hydroxy, which acted as a KOR agonist with low potency (EC_{50} = 270 nM) and medium efficacy (67% stimulation). Analysis of these data implicate the role of a hydrogen bond donor at the *o*-position not only in KOR affinity but also in KOR efficacy.

DOI: 10.1021/acschemneuro.7b00284
ACS Chem. Neurosci. 2017, 8, 2549−2557

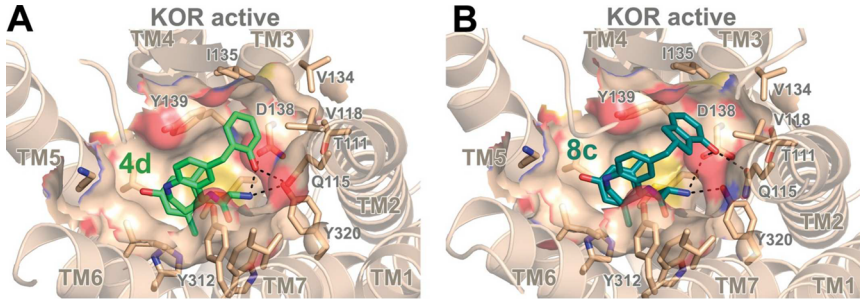

Figure 3. Compounds **4d** (A) and **8c** (B) docked in the model of the active conformation of KOR. Formation of hydrogen-bonding network between polar receptor residues and OH-groups of *o*-hydroxybenzyl pendant or 4-hydroxy-2-methylindanyl pendant could explain the increased potency and efficacy of **4d** and **8c** at KOR. Receptor helices are shown by cartoon colored beige; ligand binding pocket is shown by surface with receptor residues interacting with ligands shown by sticks colored beige for C atoms. Ligands are shown by sticks colored dark green (**4d**) and dark teal (**8c**) for C atoms. Receptor and ligand N atoms are colored blue, and O atoms are colored red.

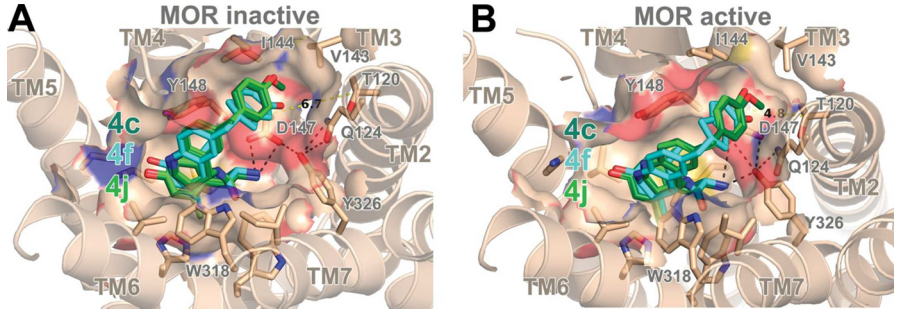

Figure 4. Overlap of compounds **4c**, **4f**, and **8d** in the binding pocket of the inactive conformation (A) and the active conformation (B) of MOR. Unfavorable interaction between polar OH-groups of *p*-hydroxybenzyl pendant or 5-hydroxy-2-methylindanyl with nonpolar microenvironment and potential presence of hydrated water near hydroxy groups prevents approach of TM3 to TM2 during activation, thus explaining the reduced efficacy of **4f** and **8d** at MOR. Receptor helices are shown by cartoon colored beige; ligand binding pocket is shown by surface with receptor residues interacting with ligands shown by sticks colored beige for C atoms. Ligands are shown by sticks colored dark green (**4c**), light green (**4f**), and cyan (**8d**) for C atoms. Receptor and ligand N atoms are colored blue, and O atoms are colored red. Distance (Å) between C^{β}-atoms of D147 and T120 residues is shown by yellow dashes with black labels.

Comparison of functional activity of compounds across all three receptors suggests that the presence of *p*-substituents at the benzyl pendant could be responsible for the notable decrease in ligand binding affinity, potency, and efficacy of **4c** and **4f** relative to **4**. Further, the inclusion of the *p*-hydroxy moiety (**4f**) was more detrimental for agonist activity of ligands at all receptors than the incorporation of a *p*-methoxy group (**4c**), which only partially reduced MOR efficacy (55% stimulation) while eliminating stimulation at DOR and KOR. These results suggest that the presence of a polar hydroxy moiety at the *p*-position is indeed a primary factor for decreased ligand efficacy at opioid receptors in this series.

In the 2-methylindanyl subseries, all analogues (**8a**–**8d**) displayed subnanomolar binding affinity at MOR and remained agonists, though with decreased MOR efficacy (16–66% maximal stimulation) compared to the unsubstituted 2-methylindanyl pendant **8** (86% stimulation). MOR efficacy of analogues with a methoxy (**8a**) or hydroxy group (**8c**) at the 4-position was less affected (48% and 66% stimulation, respectively), than efficacy of analogues with methoxy (**8b**) and hydroxy moieties (**8d**) at the 5-position (22% and 16% stimulation, respectively). Interpretation of these data aligns with methoxy and hydroxy-groups at *p*-position of benzyl pendants (**4c** and **4f**) showing a greater reduction in MOR efficacy compared to these groups in *o*- or *m*-positions. Although compounds from the 2-methylindanyl subseries (**8**, **8a**–**8d**) displayed high binding affinities to DOR, none of them activated the receptor and are therefore characterized as DOR antagonists. Interestingly, at KOR, three compounds from this subseries (**8a**, **8b**, **8d**) behaved as low affinity KOR antagonists, while the other two compounds **8** and **8c** demonstrated high binding affinities (K_i = 1.2 nM and 0.77 nM, respectively) and the ability to activate the receptor as a partial or full KOR agonist, respectively. The increased efficacy and potency at KOR of **8c**, with a 4-hydroxy-2-methylindanyl pendant (EC_{50} = 25 nM, 92% stimulation), as compared to **8** (EC_{50} = 25 nM, 38% stimulation), correlates with the increased KOR agonist properties of **4d** with *o*-hydroxybenzyl pendant (EC_{50} = 230 nM, 67% stimulation), as compared to **4** (EC_{50} = 540 nM, 22% stimulation). These results confirm the importance of the hydroxy moiety at the *o*-position of the benzyl pendant or at the 4-position of the 2-methylindanyl pendant for proper KOR binding and activation.

Modeling of Opioid Receptor–Ligand Complexes. To understand the role of the hydroxy moiety at different pendant positions for modulating agonist properties of the studied ligands, we analyzed models of KOR and MOR in complex with these ligands. Models of MOR–ligand complexes were based on recently obtained crystal structures of inactive and active states of MOR (PDB IDs 4dkl and 5c1m, respectively), while a homology model of activated KOR was built using the crystal structure of the activated MOR (PDB ID 5c1m). The ligand docking used superposition of peptidomimetics with crystallized ligands followed by complex refinement, as described in Methods.

DOI: 10.1021/acschemneuro.7b00284
ACS Chem. Neurosci. 2017, 8, 2549–2557

Modeling demonstrated that hydroxy moieties of both **4d** (*o*-hydroxybenzyl pendant) and **8c** (4-hydroxy-2-methylindanyl pendant) docked in the active conformation of KOR (Figure 3) occupy a similar spatial position near the patch of polar and charged residues from transmembrane (TM) helices 2, 3, and 7 of the receptor. The hydroxy groups of **4d** and **8c** may form extensive hydrogen bonds with polar receptor groups from residues Q115 (TM2), D138 (TM3), and Y320 (TM7), and are in proximity to Y312 (TM7). These hydrogen-bonding interactions between polar groups could explain the improved binding affinities of **4d** and **8c** to KOR and their improved propensity for stimulating receptor activation.

Comparison of binding poses of ligands **4c** (*p*-methoxybenzyl pendant), **4f** (*p*-hydroxybenzyl pendant), and **8d** (5-hydroxy-2-methylindanyl pendant) in the active and inactive conformations of MOR (Figure 4) demonstrate that the methoxy and hydroxy groups of these ligands are within the hydrophobic depression of the ligand binding pocket, which is formed by residues T120 from TM2 and V143, I144, and D147 from TM3. The hydroxy moieties of compounds **4f** and **8d** cannot form favorable hydrogen bonding interactions in the nonpolar environment of residues V143 and I144 and may remain hydrated upon binding to the receptor. The more hydrophobic *p*-methoxy group of **4c** can be better accommodated in this nonpolar microenvironment, being dehydrated. The expected water molecules from the hydration shell of hydroxy groups of **4f** or **8d** can be accommodated between residues D147 and T120 in the inactive MOR state (C^{β}–C^{β} distance 6.7 Å) but not in the active MOR state (C^{β}–C^{β} distance 4.8 Å). Thus, the presence of hydrated water would prevent receptor activation associated with TM3 movement closer to TM2 and shrinking of the hydrophobic depression enclosed by T120, V143, I144, and D147 residues. These observations could explain how hydroxy substitutions located at distal positions of the pendants yield unfavorable effects on ligand efficacy at MOR.

DISCUSSION AND CONCLUSIONS

In our recent design and SAR analysis of a series of opioid peptidomimetics based on a tetrahydroquinoline (THQ) scaffold, we defined structural features of these ligands that were beneficial for mixed-efficacy ligands targeting MOR and DOR but not KOR. In particular, we observed that modifications influencing structure and size of pendants attached to the THQ core usually improved ligand binding affinity to all opioid receptors but differently affected efficacy: ligand efficacy increased at MOR, decreased at DOR, and was variable at KOR.[11,12] We also found that *N*-acetylation and attachment of hydrophobic, carbonyl-containing *N*-substitutions to the THQ core improved binding affinity and efficacy at DOR.[11,13] As a result we have generated several peptidomimetics that exhibit MOR agonist/DOR antagonist[10−12] and MOR agonist/DOR agonist[13] pharmacological profiles and that have shown increased *in vivo* bioavailability.[11−13] These peptidomimetics, which comprise a unique structural scaffold, could serve as leads for development of refined analgesics devoid of tolerance and dependence liabilities.

In this study, by analyzing the effect of methoxy and hydroxy moieties on benzyl and 2-methylindanyl pendants attached to the THQ scaffold, we further explored properties of the opioid receptor binding pocket in the region between TM helices 2, 3, and 7, the site of binding of these pendants. Our data suggest that the placement of the methoxy and hydroxy moieties on the benzyl and 2-methylindanyl pendants greatly influences binding and efficacy profiles at both MOR and KOR. Hydroxy and methoxy substituents that extend deeply into the pendant binding pocket (like the 5-substituted-2-methylindanyl, **8b** and **8d,** and *p*-substituted benzyl, **4c** and **4f** analogues) were not well tolerated and thus decreased or eliminated binding affinity and/or efficacy at MOR. Furthermore, we identified modifications of the pendant on the THQ core that significantly improved ligand properties at KOR. In particular, KOR affinity and efficacy was largely influenced by the presence and placement of a hydrogen-bond-donating hydroxy moiety. The *o*- and *m*-hydroxybenzyl analogues (**4d** and **4e**, respectively), as well as the 4-hydroxy-2-methylindanyl analogue (**8c**), had improved ligand binding affinity at KOR, and the *o*-hydroxybenzyl (**4d**) and 4-hydroxy-2-methylindanyl (**8c**) analogues had significantly increased KOR efficacy (67% and 92%, respectively). The latter finding is particularly significant, as **8c** is the first analogue in this THQ-based series to display high affinity, potency, and efficacy both at MOR (K_i = 0.18 nM, EC_{50} = 4.9 nM, 66% stimulation) and at KOR (K_i = 0.77 nM, EC_{50} = 25 nM, 92% stimulation), while evoking no stimulation at DOR. Thus, **8c** represents a promising lead in the future development of MOR/KOR bifunctional ligands.

METHODS

Chemistry. All reagents and solvents were obtained from commercial sources and used without additional purification. Flash column chromatography was carried out using P60 silica gel (230−400 mesh) either manually or with a Biotage Isolera instrument. Before flash column chromatography was performed, crude mixtures were analyzed using thin-layer chromatography using 2:3 EA/hex, 1:1 EA/hex, or 3:2 EA/hex. The R_f values of products and impurities were calculated and then copied into either the linear gradient or the stepwise gradient wizard on the Biotage Isolera instrument. The TLC wizard then determined the optimal purification technique (all techniques started from low percentage EtOAc (0−10%) in hexanes and ending with 100% EtOAc), which was used to purify crude mixtures. Suzuki couplings were performed on a Discover S-class (CEM) microwave in a closed vessel with maximum power input of 300 W and temperature set at 110 °C for 10−60 min under the standard method from their Synergy software. Purification of final compounds was performed using a Waters semipreparative HPLC with a Vydac protein and peptide C18 reverse phase column, using a linear gradient of 0% solvent B (0.1% TFA in acetonitrile) in solvent A (0.1% TFA in water) to 100% solvent B in solvent A at a rate 1% per minute and monitoring UV absorbance at 230 nm. Purity of synthesized compounds was determined on a Waters Alliance 2690 analytical HPLC instrument and a Vydac protein and peptide C18 reverse phase column, using a linear gradient of 0% solvent B in solvent A to 45%, 70%, or 90% solvent B in solvent A in 45, 70, or 90 min, respectively, and UV absorbance at 230 nm (gradient A). Purities of the final compounds used for testing were ≥95%, unless otherwise stated, as determined by HPLC. ^{1}H NMR and ^{13}C NMR data were obtained on either a 400 or 500 MHz Varian spectrometer using $CDCl_3$ or CD_3OD solvents. The identity of each compound was verified by mass spectrometry using an Agilent 6130 LC−MS mass spectrometer in positive mode.

General Procedure A for Suzuki Coupling. Suzuki coupling was completed using a modified procedure from ref 31. A solution of 3:1 acetone/dI H_2O was degassed for 1 h, then Ar was bubbled through solution for 1 h to ensure removal and displacement of ambient oxygen. When all reagents were solids, aromatic bromide (1.0 equiv), boronic ester (2.0 equiv), K_2CO_3 (3.0 equiv), and Pd(dppf)Cl_2 (0.1 equiv) were added to a microwave tube, and the tube was placed under vacuum for 15 min, then flooded with Ar. Roughly 1−2 mL of the 3:1 acetone/dI H_2O solution was added to the tube via syringe, then tube was placed in microwave for 30−60 min with a maximum power of

DOI: 10.1021/acschemneuro.7b00284
ACS Chem. Neurosci. 2017, 8, 2549−2557

300 W and a maximum temperature of 100 °C with the "PowerMax" option enabled. When the boronic ester was a liquid, aromatic bromide (1.0 equiv), K_2CO_3 (3.0 equiv), and $Pd(dppf)Cl_2$ (0.1 equiv), were added to a microwave tube, and the tube was placed under vacuum for 15 min, then flooded with Ar. Roughly 1−2 mL of the 3:1 acetone/dI H_2O solution was added to tube via syringe, followed by addition of the boronic ester (2.0 equiv) via syringe. The tube was placed in microwave for 30−60 min with a maximum power of 300 W and a maximum temperature of 100 °C with the "PowerMax" option enabled. Once the microwave reaction was complete, the reaction mixture was filtered through a pad of Celite to remove palladium, and solvents were removed under reduced pressure to yield a crude brown residue, which was purified using silica gel chromatography to obtain the pure product.

General procedure B for the Synthesis of (*R*,*R*) THQ Sulfinamides.[24−26] To a round-bottom flask already containing dried, desiccated *N*-substituted dihydroquinolinone intermediate (1.0 equiv) was added (*R*)-2-methylpropane-2-sulfinamide (3.0 equiv), then the round-bottom flask was placed under vacuum for 10 min. Meanwhile, a reflux condenser was flame-dried under vacuum and then flooded with Ar. Next, anhyd. THF (∼20 mL) was added to the reaction vessel containing starting reagents via syringe. The reaction solution allowed to stir under vacuum for ∼5 min and then was flooded with Ar. The round-bottom flask was placed in an ice bath and allowed to equilibrate. Next, $Ti(OEt)_4$ (6.0 equiv) was added slowly via syringe. Once the addition was complete, the reaction vessel was taken out of the ice bath and placed in an oil bath at 70−75 °C, equipped with a condenser, and stirred for 16−48 h under Ar. Conversion of the ketone to the imine was monitored by TLC. Once sufficient conversion to the *tert*-butanesulfinyl imine was observed, the reaction vessel was taken out of the oil bath and cooled to ambient temperature. Meanwhile, an additional round-bottom flask containing a stir bar was flame-dried under vacuum, then flooded with Ar; then $NaBH_4$ was added quickly, and the reaction vessel was placed back under vacuum for 5 min. Minimal anhyd. THF was added (∼5 mL), and the vessel was allowed to stir under vacuum for ∼5 min, and then was flooded with Ar. The round-bottom flask was placed in a dry ice/xylenes bath and allowed to equilibrate. Contents from the round-bottom flask containing the imine intermediate were transferred to round-bottom flask containing $NaBH_4$ via cannula. Once contents were completely added, the reaction mixture was taken out of the dry ice/xylenes bath and allowed to warm to room temperature. The reaction was stirred at ambient temperature for 2−3 h. Once the reaction was complete, MeOH was added to quench. The solvent was removed under reduced pressure yielding a solid residue. The residue was resuspended in DCM, the remaining solid was removed by filtration through a cotton plug, and the mother liquor was concentrated and purified using silica gel chromatography to yield pure sulfinamide.

General Procedure C for diBoc-Dmt Coupling. To a round-bottom flask already containing sulfinamide intermediate was added 15−20 mL of dioxane followed by concd HCl (6.0 equiv). The reaction was stirred at RT for up to 3 h. Solvent was removed under reduced pressure to yield a slightly yellow, clear residue. The residue was resuspended in Et_2O. If a white solid precipitated (the HCl salt of the amine), the solid was removed via filtration as product without any further purification necessary. If a white solid did not precipitate, but residue remained as a film on the flask, the residue was washed with fresh Et_2O (3 × 5 mL) and dried without any further purification necessary. The (*R*)-amine intermediate and diBoc-Dmt (1.05 equiv) and the coupling reagents PyBOP (1.0 equiv) and HOBt-Cl (1.0 equiv) were dissolved in DMF (10−15 mL) followed by the addition of DIPEA (10.0 equiv). The reaction mixture was stirred for up to 18 h at RT. After concentration under reduced pressure, the crude residue was split into two batches. One batch was taken ahead to form the −OMe final product following general procedure D, while the other batch was taken ahead following general procedure E to form the −OH final product.

General Procedure D for Boc Deprotection of Final Product To Form the −OMe Final Products. The crude residue that resulted after following general procedure C was dissolved in a 1:1 mixture of DCM and TFA (10 mL) and stirred for 1 h. The mixture was concentrated and purified by semipreparative HPLC then lyophilized to yield the final compound with an −OMe functional group.

General Procedure E for Methoxy Ether Cleavage and Boc Deprotection To Form −OH Final Products. The crude residue that resulted after following general procedure C was treated with a 1 M solution of BBr_3 in DCM (0.375 mL, 5.0 equiv). The BBr_3 solution was slowly added to the reaction vessel containing the residue to remove the Boc groups and cleave the methyl ether. Once completely added, the solution stirred for 3 h. After the requisite 3 h, the solvent was removed under reduced pressure, and the residue was resuspended in MeOH, then the solvent was removed. This process was repeated 3 times to yield crude product, which was purified by semipreparative HPLC and lyophilized to yield the final product as a TFA salt.

General Procedure F for Boc-Protection of the THQ Nitrogen. To a flame-dried round-bottom flask under Ar was added the 2,3-dihydroquinolin-4(1*H*)-one (1.0 equiv), Boc_2O (1.2−2.0 equiv), and DMAP (0.1 equiv). The reaction vessel was placed back under vacuum for 5 min, then anhyd. DCM was added via syringe, and the solution stirred for 5 min under vacuum. The round-bottom flask was flooded with Ar, and DIPEA (1.2−2.0 equiv) was added via syringe. The reaction vessel was equipped with a condenser and placed in oil bath at 60 °C. The reaction was stirred at reflux for 12−16 h under Ar and was monitored by TLC. Once significant conversion to product was seen (as indicated by a higher R_f value on TLC), the reaction was quenched using dI H_2O (20 mL) and the layers were separated. The organic layer was washed with sat. $NaHCO_3$ solution (1 × 20 mL) and brine (1 × 20 mL), then dried over $MgSO_4$, filtered, and concentrated under reduced pressure to yield a crude yellow oil, which was purified using silica gel chromatography to obtain the pure product.

***In Vitro* Pharmacology. Cell Lines and Membrane Preparations.** All tissue culture reagents were purchased from Gibco Life Sciences (Grand Island, NY, U.S.). C6-rat glioma cells stably transfected with and overexpressing rat μ (C6-MOR) or rat δ (C6-DOR) opioid receptor[28] and Chinese hamster ovary (CHO) cells stably overexpressing human κ (CHO-KOR) opioid receptor[29] were used for all *in vitro* assays. Cells were grown to confluence at 37 °C in 5% CO_2 in Dulbecco's modified Eagle medium (DMEM) containing 10% fetal bovine serum and 5% penicillin/streptomycin. Membranes were prepared by washing confluent cells three times with ice cold phosphate buffered saline (0.9% NaCl, 0.61 mM Na_2HPO_4, 0.38 mM KH_2PO_4, pH 7.4). Cells were detached from the plates by addition of warm harvesting buffer (20 mM HEPES, 150 mM NaCl, 0.68 mM EDTA, pH 7.4) and pelleted by centrifugation at 1600 rpm for 3 min. The cell pellet was suspended in ice-cold 50 mM Tris-HCl buffer, pH 7.4, and homogenized with a Tissue Tearor (Biospec Products, Inc., Bartlesville, OK, U.S.) for 20 s. The homogenate was centrifuged at 15 000 rpm for 20 min at 4 °C. The pellet was rehomogenized with a Tissue Tearor for 10 s in fresh 50 mM Tris-HCl, followed by recentrifugation. The final pellet was resuspended in fresh 50 mM Tris-HCl and frozen in aliquots at 80 °C. Protein concentration was determined by performing a BCA protein assay (Thermo Scientific Pierce, Waltham, MA, U.S.) using bovine serum albumin as the standard.

Radioligand Binding Assays. Radiolabeled compounds were purchased from PerkinElmer (Waltham, MA, U.S.). Opioid ligand binding assays were performed by competitive displacement of 0.2 nM [^{3}H]-diprenorphine (250 μCi, 1.85 TBq/mmol) by the peptidomimetic from membrane preparations containing opioid receptors as described above. The assay mixture, containing membranes (20 μg protein/tube) in 50 mM Tris-HCl buffer (pH 7.4), [^{3}H]-diprenorphine, and various concentrations of test peptidomimetic, was incubated at room temperature for 1 h to allow binding to reach equilibrium. The samples were rapidly filtered through Whatman GF/C filters using a Brandel tissue harvester (Brandel, Gaithersburg, MD, U.S.) and washed five times with 50 mM Tris-HCl buffer. Bound

DOI: 10.1021/acschemneuro.7b00284
ACS Chem. Neurosci. 2017, 8, 2549−2557

radioactivity on dried filters was determined by liquid scintillation counting, after saturation with EcoLume liquid scintillation cocktail, in a Wallac 1450 MicroBeta (PerkinElmer, Waltham, MA, U.S.). Nonspecific binding was determined using 10 μM naloxone. The results presented are the mean ± standard error (SEM) from at least three separate assays performed in duplicate. K_i (nM) values were calculated using nonlinear regression analysis to fit a logistic equation to the competition data using GraphPad Prism, version 6.0c, for Mac OS X (GraphPad Software Inc., La Jolla, CA).

Stimulation of [^{35}S]-GTPγS Binding. Agonist stimulation of [^{35}S]guanosine 5′-O-[γ-thio]triphosphate ([^{35}S]-GTPγS, 1250 Ci, 46.2 TBq/mmol) binding to G-protein was measured as described previously.[30] Briefly, membranes (10−20 μg of protein/tube) were incubated 1 h at 25 °C in GTPγS buffer (50 mM Tris-HCl, 100 mM NaCl, 5 mM $MgCl_2$, pH 7.4) containing 0.1 nM [^{35}S]-GTPγS, 30 μM guanosine diphosphate (GDP), and varying concentrations of test peptidomimetic. G protein activation following receptor stimulation of [^{35}S]-GTPγS (% stimulation) with peptidomimetic was compared with 10 μM of the standard compounds [D-Ala2,N-MePhe4,Gly-ol]-enkephalin (DAMGO) at MOR, D-Pen2,5-enkephalin (DPDPE) at DOR, or U69,593 at KOR. The reaction was terminated by vacuum filtration of GF/C filters that were washed 10 times with GTPγS buffer. Bound radioactivity was measured as described above. The results are presented as the mean ± standard error (SEM) from at least three separate assays performed in duplicate; potency (EC_{50} (nM)) and % stimulation values were determined using nonlinear regression analysis with GraphPad Prism, same as above.

Computational Modeling. Three-dimensional (3D) models of opioid receptors in the inactive conformation were produced as previously described[32] using X-ray structures of the mouse MOR in the inactive (PDB ID 4dkl)[33] and the active (PDB ID 5c1m)[34] conformations. The latter template was used for homology modeling of active conformations of KOR. Structures of KOR loops in the active state were kept consistent with those in the crystal structures of the inactive state (PDB ID 4djh).[35] The N-terminus of KOR (residues 45−57) was modeled in the extended conformation of the polypeptide chain lacking the bulge present in the N-terminus of MOR template. Such modifications increased the size of the binding pocket and allowed docking of peptidomimetics without hindrance of the N-terminus. Structures of peptidomimetic ligands were generated using the 3D-Builder Application of QUANTA (Accelrys, Inc.) followed by Conformational Search included in the program package. Low-energy ligand conformations (within 2 kcal/mol) that demonstrated the best superposition of aromatic substituents of the THQ core with the pharmacophore elements (Tyr^1 and Phe^3) of receptor-bound conformations of cyclic tetrapeptides[36,37] were selected for docking into the receptor binding pocket. Thus, only one stereoisomer of compounds from the 2-methylindanyl subseries with best fit to the tetrapeptide structure was chosen (see Figures 3 and 4). Ligands were positioned inside the receptor binding cavity to reproduce the binding modes of cyclic tetrapeptides and crystallized ligands in structural templates. The docking pose of each ligand was subsequently refined using the solid docking module of QUANTA. The receptor−ligand complexes were then minimized with CHARMm implemented in QUANTA (Adopted-Basis Newton−Raphson method, 50 steps, ε = 10). Models of opioid ligand−receptor complexes are available upon request.

■ ASSOCIATED CONTENT

Supporting Information

The Supporting Information is available free of charge on the ACS Publications website at DOI: 10.1021/acschemneuro.7b00284.

Detailed descriptions of experimental setups for reactions with references and compound characterization of intermediates (PDF)

■ AUTHOR INFORMATION

Corresponding Author

*H.I.M. E-mail: him@umich.edu.

ORCID

Henry I. Mosberg: 0000-0002-4107-8870

Author Contributions

Aubrie A. Harland designed and synthesized the compounds described here. Irina D. Pogozheva performed molecular modeling and docking studies. Nicholas W. Griggs planned and performed in vitro pharmacology studies. Tyler J. Trask performed in vitro pharmacology. John R. Traynor oversaw all in vitro pharmacology. Henry I. Mosberg planned and oversaw study.

Funding

This study was supported by NIH Grant DA003910 (H.I.M. and J.R.T.).

Notes

The authors declare no competing financial interest.

■ ABBREVIATIONS

DAMGO, [D-Ala2,N-MePhe4,Gly-ol]enkephalin; dI H_2O, deionized water; DIPEA, diisopropyl ethyl amine; DMF, dimethylformamide; DOR, delta opioid receptor; DPDPE, D-Pen2,5-enkephalin; GDP, guanosine diphosphate; [^{35}S]GTPγS, [^{35}S]guanosine 5′-O-[γ-thio]triphosphate; KOR, kappa opioid receptor; MOR, mu opioid receptor; TFA, trifluoroacetic acid; TfOH, trifluoromethanesulfonic acid; THN, tetrahydronaphthalene; THQ, tetrahydroquinoline

■ REFERENCES

(1) Abdelhamid, E. E., Sultana, M., Portoghese, P. S., and Takemori, A. E. (1991) Selective blockage of the delta opioid receptors prevents the development of morphine tolerance and dependence in mice. *J. Pharmacol. Exp. Ther. 258*, 299−303.

(2) Fundytus, M. E., Schiller, P. W., Shapiro, M., Weltrowska, G., and Coderre, T. J. (1995) Attenuation of morphine tolerance and dependence with the highly selective delta opioid receptor antagonist TIPP(psi). *Eur. J. Pharmacol. 286*, 105−108.

(3) Hepburn, M. J., Little, P. J., Gringas, J., and Khun, C. M. (1997) Differential effects of naltrindole on morphine-induced tolerance and physical dependence in rats. *J. Pharmacol. Exp. Ther. 281*, 1350−1356.

(4) Ananthan, S. (2006) Opioid ligands with mixed mu/delta opioid receptor interactions: an emerging approach to novel analgesics. *AAPS J. 8*, E118−E125.

(5) Lowery, J. J., Raymond, T. J., Giuvelis, D., Bidlack, J. M., Polt, R., and Bilsky, E. J. (2011) In vivo characterization of MMP-2200, a mixed delta/mu opioid agonist, in mice. *J. Pharmacol. Exp. Ther. 336*, 767−778.

(6) Mello, N. K., Mendelson, J. H., Sholar, M. B., Jaszyna-Gasior, M., Goletiani, N., and Siegel, A. J. (2005) Effects of the mixed Mu /Kappa opioid nalbuphine on cocaine- induced changes in subjective and cardiovascular responses in men. *Neuropsychopharmacology 30*, 618−632.

(7) Di Chiara, G., and Imperato, A. (1988) Opposite effects of mu and kappa opiate agonists on dopamine release in the nucleus accumbens and in the dorsal caudate of freely moving rats. *J. Pharmacol. Exp. Ther. 244*, 1067−1080.

(8) Rech, R. H., Mokler, D. J., and Briggs, S. L. (2012) Effects of combined opioids on pain and mood in mammals. *Pain Res. Treat. 2012*, 145965.

(9) Varadi, A., Marrone, G. F., Eans, S. O., Ganno, M. L., Subrath, J. J., Le Rouzic, V., Hunkele, A., Pasternak, G. W., McLaughlin, J. P., and Majumdar, S. (2015) Synthesis and characterization of a dual kappa-delta opioid receptor agonist analgesic blocking cocaine reward behavior. *ACS Chem. Neurosci. 6*, 1813−1824.

DOI: 10.1021/acschemneuro.7b00284
ACS Chem. Neurosci. 2017, 8, 2549−2557

(10) Mosberg, H. I., Yeomans, L., Harland, A. A., Bender, A. M., Sobczyk-Kojiro, K., Anand, J. P., Clark, M. J., Jutkiewicz, E. M., and Traynor, J. R. (2013) Opioid peptidomimetics: leads for the design of bioavailable mixed efficacy μ opioid receptor (MOR) agonist/δ opioid receptor (DOR) antagonist ligands. *J. Med. Chem. 56*, 2139−2149.
(11) Harland, A. A., Yeomans, L., Griggs, N. W., Anand, J. P., Pogozheva, I. D., Jutkiewicz, E. M., Traynor, J. R., and Mosberg, H. I. (2015) Further optimization and evaluation of bioavailable, mixed-efficacy mu-opioid receptor (MOR) agonists/delta-opioid Receptor (DOR) antagonists: balancing MOR and DOR affinities. *J. Med. Chem. 58*, 8952−8969.
(12) Bender, A. M., Griggs, N. W., Anand, J. P., Traynor, J. R., Jutkiewicz, E. M., and Mosberg, H. I. (2015) Asymmetric synthesis and in vitro and in vivo activity of tetrahydroquinolines featuring a diverse set of polar substitutions at the 6 position as mixed-efficacy μ opioid receptor/δ opioid receptor ligands. *ACS Chem. Neurosci. 6*, 1428−1435.
(13) Harland, A. A., Bender, A. M., Griggs, N. W., Gao, C., Anand, J. P., Pogozheva, I. D., Traynor, J. R., Jutkiewicz, E. M., and Mosberg, H. I. (2016) Effects of N-substitutions on the tetrahydroquinoline (THQ) core of mixed-efficacy mu opioid receptor (MOR)/delta opioid receptor (DOR) ligands. *J. Med. Chem. 59*, 4985−4998.
(14) Thomas, J. B., Atkinson, R. N., Rothman, R. B., Fix, S. E., Mascarella, S. W., Vinson, N. A., Xu, H., Dersch, C. M., Lu, Y.-F., Cantrell, B. E., Zimmerman, D. M., and Carroll, F. I. (2001) Identification of the first trans-(3*R*,4*R*)-dimethyl-4-(3-hydroxyphenyl)-piperidine derivative to possess highly potent and selective opioid kappa receptor antagonist activity. *J. Med. Chem. 44*, 2687−2690.
(15) Lahti, R. A., Mickelson, M. M., McCall, J. M., and Von Voigtlander, P. F. (1985) [3H]U-69593 A highly selective ligand for the kappa opioid receptor. *Eur. J. Pharmacol. 109*, 281−284.
(16) Frankowski, K. J., Hedrick, M. P., Gosalia, P., Li, K., Shi, S., Whipple, D., Ghosh, P., Prisinzano, T. E., Schoenen, F. J., Su, Y., Vasile, S., Sergienko, E., Gray, W., Hariharan, S., Milan, L., Heynen-Genel, S., Mangravita-Novo, A., Vicchiarelli, M., Smith, L. H., Streicher, J. M., Caron, M. G., Barak, L. S., Bohn, L. M., Chung, T. D. Y., and Aubé, J. (2012) Discovery of small molecule kappa opioid receptor agonist and antagonist chemotypes through a HTS and hit refinement strategy. *ACS Chem. Neurosci. 3*, 221−236.
(17) Frankowski, K. J., Ghosh, P., Setola, V., Tran, T. B., Roth, B. L., and Aubé, J. (2010) N-alkyl-octahydroisoquinolin-1-one-8-carboxamides: selective and nonbasic κ-opioid receptor ligands. *ACS Med. Chem. Lett. 1*, 189−193.
(18) Spetea, M., Berzetei-Gurske, I., Guerrieri, E., and Schmidhammer, H. (2012) Discovery and pharmacological evaluation of a diphenethylamine derivative (HS665), a highly potent and selective κ opioid receptor agonist. *J. Med. Chem. 55*, 10302−10306.
(19) Spetea, M., Eans, S. O., Ganno, M. K., Lantero, A., Mairegger, M., Toll, L., Schmidhammer, H., and McLaughlin, J. P. (2017) Selective K receptor partial agoanist HS666 produces potent antinociception without inducing aversion after i.c.v. administration in mice. *Br. J. Pharmacol. 174*, 2444−2456.
(20) Williams, D. A., Zheng, Y., David, B. G., Yuan, Y., Zaidi, S. A., Stevens, D. L., Scoggins, K. L., Selley, D. E., Dewey, W. L., Akbarali, H. I., and Zhang, Y. (2016) 6β-N-Heterocyclic substituted naltrexamine derivative BNAP: a peripherally selective mixed MOR/KOR Ligand. *ACS Chem. Neurosci. 7*, 1120−1129.
(21) Deb, I., Paira, P., Hazra, A., Banerjee, S., Dutta, P. K., Mondal, N. B., and Das, S. (2009) Synthesis and characterizations of novel quinoline derivatives having mixed ligand activities at the κ and μ receptors: potential therapeutic efficacy against morphine dependence. *Bioorg. Med. Chem. 17*, 5782−5790.
(22) Greedy, B. M., Bradbury, F., Thomas, M. P., Grivas, K., Cami-Kobeci, G., Archambeau, A., Bosse, K., Clark, M. J., Aceto, M., Lewis, J. W., Traynor, J. R., and Husbands, S. M. (2013) Orvinols with Mixed Kappa/Mu Opioid Receptor Agonist Activity. *J. Med. Chem. 56*, 3207−3216.
(23) Zhou, L., Lovell, K. M., Frankowski, K. J., Slauson, S. R., Phillips, A. M., Streicher, J. M., Stahl, E., Schmid, C. L., Hodder, P., Madoux, F., Cameron, M. D., Prisinzano, T. E., Aubé, J., and Bohn, L. M. (2013) Development of functionally selective, small molecule agonists at kappa opioid receptors. *J. Biol. Chem. 288*, 36703−36716.
(24) Tanuwidjaja, J., Peltier, H. M., and Ellman, J. A. (2007) One-pot asymmetric synthesis of either diastereomer of tert-butanesulfinyl-protected amines from ketones. *J. Org. Chem. 72*, 626−629.
(25) Borg, G., Cogan, D. A., and Ellman, J. A. (1999) One-pot asymmetric synthesis of tert-butanesulfinyl-protected amines from ketones by the in situ reduction of tert-butanesulfinyl ketimines. *Tetrahedron Lett. 40*, 6709−6712.
(26) Colyer, J. T., Andersen, N. G., Tedrow, J. S., Soukup, T. S., and Faul, M. M. (2006) Reversal of diastereofacial selectivity in hydride reductions of N-tert-butanesulfinyl imines. *J. Org. Chem. 71*, 6859−6862.
(27) Schmidt, R. G., Bayburt, E. K., Latshaw, S. P., Koenig, J. R., Daanen, J. F., McDonald, H. A., Bianchi, B. R., Zhong, C., Joshi, S., Honore, P., Marsh, K. C., Lee, C. H., Faltynek, C. R., and Gomtsyan, A. L. (2011) Chroman and tetrahydroquinoline ureas as potent TRPV1 antagonists. *Bioorg. Med. Chem. Lett. 21*, 1338−1341.
(28) Lee, K. O., Akil, H., Woods, J. H., and Traynor, J. R. (1999) Differential binding properties of oripavines at cloned mu- and delta-opioid receptors. *Eur. J. Pharmacol. 378*, 323−330.
(29) Husbands, S. M., Neilan, C. L., Broadbear, J., Grundt, P., Breeden, S., Aceto, M. D., Woods, J. H., Lewis, J. W., and Traynor, J. R. (2005) BU74, a complex oripavine derivative with potent kappa opioid receptor agonism and delayed opioid antagonism. *Eur. J. Pharmacol. 509*, 117−125.
(30) Traynor, J. R., and Nahorski, S. R. (1995) Modulation by mu-opioid agonists of guanosine-5′-O(3-[35S]thio)triphosphate binding to membranes from human neuroblastoma SHY5Y cells. *J. Mol. Pharmacol. 47*, 848−854.
(31) Bandgar, B. P., Bettigeri, S. V., and Phopase, J. J. (2004) Palladium catalyzed ligand-free Suzuki cross-coupling reactions of benzylic halides with aryl boronic acids under mild conditions. *Tetrahedron Lett. 45*, 6959−6962.
(32) Anand, J. P., Purington, L. C., Pogozheva, I. D., Traynor, J. R., and Mosberg, H. I. (2012) Modulation of opioid receptor ligand affinity and efficacy using active and inactive state receptor models. *Chem. Biol. Drug Des. 80*, 763−770.
(33) Manglik, A., Kruse, A. C., Kobilka, T. S., Thian, F. S., Mathiesen, J. M., Sunahara, R. K., Pardo, L., Weis, W. I., Kobilka, B. K., and Granier, S. (2012) Crystal structure of the μ-opioid receptor bound to a morphinan antagonist. *Nature 485*, 321−326.
(34) Huang, W., Manglik, A., Venkatakrishnan, A. J., Laeremans, T., Feinberg, E. N., Sanborn, A. L., Kato, H. E., Livingston, K. E., Thorsen, T. S., Kling, R. C., Granier, S., Gmeiner, P., Husbands, S. M., Traynor, J. R., Weis, W. I., Steyaert, J., Dror, R. O., and Kobilka, B. K. (2015) Structural insights into m-opioid receptor activation. *Nature 524*, 315−321.
(35) Wu, H., Wacker, D., Mileni, M., Katritch, V., Han, G. W., Vardy, E., Liu, W., Thompson, A. A., Huang, X.-P., Carroll, F. I., Mascarella, S. W., Westkaemper, R. B., Mosier, P. D., Roth, B. L., Cherezov, V., and Stevens, R. C. (2012) Structure of the human κ-opioid receptor in complex with JDTic. *Nature 485*, 327−332.
(36) Fowler, C. B., Pogozheva, I. D., Lomize, A. L., LeVine, H., and Mosberg, H. I. (2004) Complex of an active μ-opioid receptor with a cyclic peptide agonist modeled from experimental constraints. *Biochemistry 43*, 15796−15810.
(37) Pogozheva, I. D., Przydzial, M. J., and Mosberg, H. I. (2005) Homology modeling of opioid receptor-ligand complexes using experimental constraints. *AAPS J. 7*, E434−448.

DOI: 10.1021/acschemneuro.7b00284
ACS Chem. Neurosci. 2017, 8, 2549−2557